MOX–Report No. 30/2014

Numerical analysis of Darcy problem on surfaces

Ferroni, A.; Formaggia, L.; Fumagalli, A.;

MOX, Dipartimento di Matematica "F. Brioschi"
Politecnico di Milano, Via Bonardi 9 - 20133 Milano (Italy)

lab-mox@polimi.it http://mox.polimi.it

Numerical analysis of Darcy problem on surfaces

Alberto Ferroni[♯], Luca Formaggia[♯] and Alessio Fumagalli[♯]

July 17, 2014

[♯] MOX– Modellistica e Calcolo Scientifico
Dipartimento di Matematica "F. Brioschi"
Politecnico di Milano
via Bonardi 9, 20133 Milano, Italy
alberto.ferroni@polimi.it
luca.formaggia@polimi.it
alessio.fumagalli@mail.polimi.it

Keywords: PDEs on surfaces, Darcy problem, Mixed finite elements.

AMS Subject Classification:65N30,65N15,76S05

Abstract

Surface problems play a key role in several theoretical and applied fields. In this work the main focus is the presentation of a detailed analysis of the approximation of the classical flow porous media problem: the Darcy equation, where the domain is a regular surface. The formulation require the mixed form and the numerical approximation consider the classical pair of finite element spaces: piecewise constant for the scalar fields and Raviart-Thomas for vector fields, both written on the tangential space of the surface. The main result is the proof of the order of convergence where the discretization error, due to the finite element approximation, is coupled with a geometrical error. The latter takes into account the approximation of the real surface with a discretized one. Several examples are presented to show the correctness of the analysis, including surfaces without boundary.

1 Introduction

In several application, like biology [5] or geophysics, the domains where some or part of problems have to be solved are surfaces or lines. In this particular framework several works in literature are present, mainly focused on the derivation and approximation of diffusive processes. Normally the resulting mathematical equations considered involve the classical Laplace-Beltrami operator [9]. A numerical approximation of this problems is presented in [3, 8, 10, 1] where standard Lagrangian finite element spaces are considered.

With this choice only the primary unknown field is computed directly, while a possible secondary unknown, like the tangential gradients, should be computed as a post process, often resulting in a poor approximation [4]. In some applications, *e.g.* in geophysics, the most important unknowns are often the secondary ones, that represent the fluxes or a macroscopic velocity, which play as a transport for advected quantities. Consequently, we are interested in problems where both the primary and secondary unknowns are computed directly. This is possible by employing a mixed formulation of the differential problem.
An important example of this choice, which is part of the motivations of the present paper, are presented in [17, 6, 16, 13, 15]. In this series of papers a reduced model is considered to approximate the flow and pressure fields in fractures. The fractures are represented as object of co-dimension one and the reduced models considered are Darcy-type equations written in the tangential spaces of each fracture. Assuming that the porous matrix is impervious, like in [13], the resulting problem is only written for the fractures.
In this work we propose and analyse a mathematical approach to the formulation of Darcy problems on surfaces embedded in $\mathbb{R}^3$. The main part of the paper is devoted to the derivation of a proper framework for the numerical approximation of such problems. The finite element spaces considered are the classical piecewise constant for scalar fields and Raviart-Thomas for vector fields, but projected on the approximate surface. Particular attention is devoted to the well posedness of the resulting discrete problem and to prove the order of convergence including also the geometrical error in the estimation. We allow the surface to be closed so no boundary conditions can be imposed and than suitable additional conditions should taking into consideration, such as zero-mean pressure or fixing the value of the latter in a point of the mesh.
The paper is organized as follow. Section 2 introduces the notations used in the paper as well as the physical problem with some assumptions on the data. The weak formulation of the physical problem and the correct functional setting is described in Section 3, where also the inf-sup condition is proved. Section 4 introduces, describes and analyses the numerical approximation where the discrete inf-sup condition is presented. An error estimation, from the chosen discretization, is derived in Section 5. In Section 6 a collection of examples highlights the potentiality of the proposed methods and the gives a numerical validation of the derived theoretical results. Finally, Section 7 is devoted to the conclusions.

2 The governing equations

We assume that the physical domain Γ is a C^2 compact, connected orientable manifold embedded in $\mathbb{R}^3$ described by a signed distance function $d : \mathbb{R}^3 \to \mathbb{R}$ such that

$$\Gamma = \{\boldsymbol{x} \in U \,:\, d(\boldsymbol{x}) = 0\},$$

where U is an open subset of $\mathbb{R}^3$ containing Γ. The outward-pointing normal is defined as $\boldsymbol{n}(\boldsymbol{x}) := \nabla d(\boldsymbol{x}) / |\nabla d(\boldsymbol{x})|$,where $\nabla d(\boldsymbol{x}) \neq 0$ almost everywhere on Γ. An other quantity that will be useful afterwards is the Hessian matrix H of the distance function d, where $H_{ij} := \frac{\partial^2 d}{\partial x_i \partial x_j}$.
In the sequel, given a function $u : \Gamma \to \mathbb{R}$, we will indicate its lifting, on a given open set U containing Γ, as $\tilde{u}$ such that $\tilde{u}|_\Gamma = u$. The tangential gradient of u will be then defined as

$$\nabla_\Gamma u := \nabla \tilde{u} - (\nabla \tilde{u} \cdot \boldsymbol{n})\, \boldsymbol{n}. \tag{1}$$

Introducing $P = I - \boldsymbol{n} \otimes \boldsymbol{n}$, where $\otimes$ is the tensor product $(\boldsymbol{a} \otimes \boldsymbol{b})_{ij} = a_i b_j$, we can rewrite (1) as $\nabla_\Gamma u = P \nabla \tilde{u}$. The definition of the tangential divergence is now straightforward, in fact a smooth given vector field $\boldsymbol{u} : \Gamma \to \mathbb{R}^3$ we have $\nabla_\Gamma \cdot \boldsymbol{u} := P : \nabla \tilde{\boldsymbol{u}}$.
The problem we are interested to solve is the classical Darcy problem [2] defined on the regular surface Γ. The two unknowns are the tangential Darcy velocity $\boldsymbol{u}$ and the pressure p. The problem is defined in the following way

$$\begin{cases} \eta \boldsymbol{u} + \nabla_\Gamma p = \boldsymbol{g} & \text{in } \Gamma \\ \nabla_\Gamma \cdot \boldsymbol{u} = f & \text{in } \Gamma \\ p = \hat{p} & \text{on } \gamma^D \\ \boldsymbol{u} \cdot \boldsymbol{\mu} = b & \text{on } \gamma^N \end{cases}, \tag{2}$$

where $\boldsymbol{\mu}$ is the outward unit normal of $\partial\Gamma$. The main data in (2) is the inverse of the permeability, defined as

$$\eta \in L^\infty(\Gamma) \quad \text{and} \quad \exists \eta_{\min} \in \mathbb{R}^+ : \eta(\boldsymbol{x}) > \eta_{\min} \geq 0 \quad \forall \boldsymbol{x} \in \Gamma. \tag{3}$$

We set $\eta_{\max} = \operatorname{supess}_{\boldsymbol{x} \in \Gamma} \eta(\boldsymbol{x})$. Moreover the scalar source term is defined as $f \in L^2(\Gamma)$ and the boundary conditions are imposed on the Darcy velocity $\boldsymbol{u}$ and on the pressure p. In the former case we consider the function b while for the latter we have the function $\hat{p}$. Finally the vector field $\boldsymbol{g}$ may represent a gravity term and the scalar field f may be viewed as a source or a sink. In the forthcoming analysis, to ease the presentation, we will assume that some of the aforementioned data are zero.

3 Weak formulation and functional setting

For simplicity we consider Dirichlet homogeneous boundary conditions, otherwise a lifting technique should be used to impose the boundary data. We introduce the weak formulation of problem (2), defining a suitable functional setting. First we introduce the functional space defined on the manifold Γ with its related norm

$$\boldsymbol{H}_{\mathrm{div}}(\Gamma) := \left\{ \boldsymbol{v} \in \left[L^2(\Gamma)\right]^3, \nabla_\Gamma \cdot \boldsymbol{v} \in L^2(\Gamma) \right\}$$

and the norm is

$$\|\boldsymbol{v}\|_{\mathrm{div},\Gamma}^2 := \|\boldsymbol{v}\|_{0,\Gamma}^2 + \|\nabla_\Gamma \cdot \boldsymbol{v}\|_{0,\Gamma}^2,$$

where $\|\cdot\|_{0,A}$ is the L^2 norm on the regular domain A. In the sequel it will be useful to introduce the standard scalar product in $L^2(A)$, with A a regular domain, as $(\cdot,\cdot)_A$. We set the functional space and the norm for the velocity as $\boldsymbol{W}$, namely

$$\boldsymbol{W} := \left\{\boldsymbol{v} \in \boldsymbol{H}_{\mathrm{div}}(\Gamma),\ \boldsymbol{v}\cdot\boldsymbol{n} = 0 \text{ on } \Gamma, \boldsymbol{v}\cdot\boldsymbol{\mu} = 0 \text{ on } \gamma^N\right\} \quad \text{with} \quad \|\boldsymbol{v}\|_{\boldsymbol{W}} := \|\boldsymbol{v}\|_{\mathrm{div},\Gamma}.$$

For the pressure field we consider the standard L^2 space with its classical norm, we have

$$Q := L^2(\Gamma) \quad \text{with} \quad \|q\|_Q = \|q\|_{0,\Gamma}.$$

If $\left|\gamma^D\right| = 0$ to recover the uniqueness of the solution, we consider the following space for the pressure field

$$Q := L_0^2(\Gamma) = \left\{v \in L^2(\Gamma) : (v,1)_\Gamma = 0\right\} \quad \text{with} \quad \|q\|_Q = \|q\|_{0,\Gamma},$$

otherwise the solution is uniquely defined in the quotient space $L^2(\Gamma)/\mathbb{R}$.
The weak formulation of the problem (2) is quite standard except the integration by part of the tangential gradient of the pressure. Taking a test function $\boldsymbol{v} \in \boldsymbol{W}$ and considering the boundary conditions, the pressure gradient term becomes

$$\int_\Gamma \nabla_\Gamma p \cdot \boldsymbol{v} \mathrm{d}x = -\int_\Gamma p \nabla_\Gamma \cdot \boldsymbol{v} \mathrm{d}x - \int_\Gamma \mathcal{K} p\, \boldsymbol{v}\cdot\boldsymbol{n} H \mathrm{d}x + \int_{\partial\Gamma} \hat{p} \boldsymbol{v}\cdot\boldsymbol{\mu} \mathrm{d}\sigma,$$

where $\mathcal{K} = \nabla_\Gamma \cdot \boldsymbol{n}$. The term which involves the matrix Hessian H is zero since we have required that $\boldsymbol{v}\cdot\boldsymbol{n} = 0$. We introduce the bilinear forms $a(\cdot,\cdot) : \boldsymbol{W}\times\boldsymbol{W} \to \mathbb{R}$ and $b(\cdot,\cdot) : \boldsymbol{W} \times Q \to \mathbb{R}$, defined as

$$a(\boldsymbol{u},\boldsymbol{v}) := (\eta\boldsymbol{u},\boldsymbol{v})_\Gamma\,, \quad \text{and} \quad b(\boldsymbol{v},q) := -\left(p, \nabla_\Gamma \cdot \boldsymbol{v}\right)_\Gamma$$

The functionals are $F(\cdot) : Q \to \mathbb{R}$ and $G(\cdot) : \boldsymbol{W} \to \mathbb{R}$, defined as

$$F(q) := -\left(f,q\right)_\Gamma . \quad \text{and} \quad G(\boldsymbol{v}) := -\left(\hat{p}, \boldsymbol{v}\cdot\boldsymbol{\mu}\right)_{\partial\Gamma} + (\boldsymbol{g},\boldsymbol{v})_\Gamma\,.$$

The weak formulation of problem (2) is presented in Problem 1.

Problem 1 (Weak formulation) *Given η as in (3), find $(\boldsymbol{u},p) \in \boldsymbol{W}\times Q$ such that*

$$\begin{cases} a(\boldsymbol{u},\boldsymbol{v}) + b(\boldsymbol{v},p) = G(\boldsymbol{v}) & \forall \boldsymbol{v} \in \boldsymbol{W} \\ b(\boldsymbol{u},q) = F(q) & \forall q \in Q \end{cases}. \tag{4}$$

Theorem 3.1 (Well posedness) *Under the given hypotheses on the data, Problem* (1) *is well posed.*

Proof. To ease the presentation we suppose that $\hat{p}$ and $\boldsymbol{g}$ are zero. However a similar result can be obtained with different constants. Since (4) is a saddle-point problem we have to prove the inf-sup condition [4, 12]. By hypothesis we have two positive constants $\eta_{\min}$ and $\eta_{\max}$ such that $\eta_{\min} \leq |\eta| \leq \eta_{\max}$ almost everywhere in Γ.
We consider the functional space $\boldsymbol{W}_0 = \{\boldsymbol{v} \in \boldsymbol{W},\, b(\boldsymbol{v}, q) = 0\, \forall q \in Q\}$ and we introduce $\boldsymbol{v} \in \boldsymbol{W}_0$. Then we have $\nabla_\Gamma \cdot \boldsymbol{v} = 0$ almost everywhere in $\boldsymbol{W}_0$ and for each function in $\boldsymbol{W}_0$ the relation $\|\boldsymbol{v}\|_{\boldsymbol{W}} = \|\boldsymbol{v}\|_{L^2(\Gamma)}$ holds true. Using these results we can prove the coercivity of $a(\cdot,\cdot)$

$$a(\boldsymbol{u}, \boldsymbol{u}) = (\eta \boldsymbol{u}, \boldsymbol{u})_\Gamma \geq \eta_{\min} \|\boldsymbol{u}\|^2_{L^2(\Gamma)} = \eta_{\min} \|\boldsymbol{u}\|^2_{\boldsymbol{W}} \quad \forall \boldsymbol{u} \in \boldsymbol{W}_0.$$

Then, thanks to the hypothesis on η and the Schwarz inequality we have the continuity of the bilinear form $a(\cdot,\cdot)$

$$|a(\boldsymbol{u}, \boldsymbol{v})| \leq \eta_{\max} \|\boldsymbol{u}\|_W \|\boldsymbol{v}\|_W \qquad \forall \boldsymbol{u}, \boldsymbol{v} \in \boldsymbol{W}.$$

Similarly for the bilinear form $b(\cdot,\cdot)$ we obtain its continuity simply using the Schwarz inequality

$$|b(\boldsymbol{v}, q)| \leq \|\nabla_\Gamma \cdot \boldsymbol{v}\|_{L^2(\Gamma)} \|q\|_{L^2(\Gamma)} \leq \|\boldsymbol{v}\|_{\boldsymbol{W}} \|q\|_Q \qquad \forall (\boldsymbol{v}, q) \in \boldsymbol{W} \times Q.$$

Finally we need to prove the inf-sup condition, *i.e.* there exists a positive constant $\beta \in \mathbb{R}^+$ such that

$$\forall q \in Q, \exists \boldsymbol{v} \in \boldsymbol{W} \qquad b(\boldsymbol{v}, q) \geq \beta \|\boldsymbol{v}\|_{\boldsymbol{W}} \|q\|_Q.$$

Given a function $q \in Q$ we consider the following auxiliary problem

$$\begin{cases} -\nabla_\Gamma \cdot (\nabla_\Gamma \varphi) = q & \text{in } \Gamma \\ \varphi = 0 & \text{on } \gamma^D \\ \nabla_\Gamma \varphi \cdot \boldsymbol{\mu} = 0 & \text{on } \gamma^N \end{cases} . \tag{5}$$

Problem (5) admits a unique solution $\varphi \in H^2(\Gamma)$ such that $\|\varphi\|_{H^2(\Gamma)} \leq C \|q\|_{L^2(\Gamma)}$. Choosing $\boldsymbol{v} = \nabla_\Gamma \varphi$, from Problem (5) we have $-\nabla_\Gamma \cdot \boldsymbol{v} = q$. Considering the aforementioned results, the following inequality holds true

$$\begin{aligned} \|\boldsymbol{v}\|^2_{\boldsymbol{W}} = \|\boldsymbol{v}\|^2_{L^2(\Gamma)} + \|\nabla_\Gamma \cdot \boldsymbol{v}\|^2_{L^2(\Gamma)} = \|\nabla_\Gamma \varphi\|^2_{L^2(\Gamma)} + \|q\|^2_{L^2(\Gamma)} \leq \\ \leq \|\varphi\|^2_{H^2(\Gamma)} + \|q\|^2_{L^2(\Gamma)} \leq (C+1) \|q\|^2_{L^2(\Gamma)}. \end{aligned}$$

Imposing $C^* = (C+1)^{\frac{1}{2}}$ we finally obtain the inf-sup condition

$$b(\boldsymbol{v}, q) = -\left(q, \nabla_\Gamma \cdot \boldsymbol{v}\right)_\Gamma = \|q\|^2_{L^2(\Gamma)} \geq \frac{1}{C^*} \|\boldsymbol{v}\|_{\boldsymbol{W}} \|q\|_Q,$$

providing $\beta = 1/C^*$. Thanks to this results we can conclude that (1) is well posed. $\square$

4 Numerical discretization

To provide a discrete formulation for Problem (1) we have to introduce a suitable approximation of the surface Γ. Following the approach presented in [9], we consider a polyhedral surface Γ_h consisting in the union of non overlapping triangles K, with vertices lying on Γ. We also require the resulting grid to be conforming and regular.
Unlike the classical finite elements method, the discrete domain Γ_h will not in general be included in Γ, thus adding to the approximation error a component that accounts for the error introduced by the discretization of the geometry. To ensure a sufficiently good approximation of the surface Γ we assume $\Gamma_h \subset U$, where U is a strip of width $\delta > 0$ in which the decomposition

$$\boldsymbol{x} = \boldsymbol{a}(\boldsymbol{x}) + d(\boldsymbol{x})\boldsymbol{n}(\boldsymbol{x}) \quad \boldsymbol{x} \in U, \tag{6}$$

is unique, being $\boldsymbol{a} : U \to \Gamma$ a projection function, d the distance of $\boldsymbol{x}$ from Γ and $\boldsymbol{n}$ its normal. Thanks to the regularity of the surface there exists a δ such that (6) holds.
We set the finite element spaces accordingly with the previous section. We start defining the space $\boldsymbol{H}_{\text{div}}(\Gamma_h)$ as

$$\boldsymbol{H}_{\text{div}}(\Gamma_h) := \{\boldsymbol{v}_h \in [L^2(\Gamma_h)]^3, \nabla_{\Gamma_h} \cdot \boldsymbol{v}_h \in L^2(\Gamma_h)\}.$$

Then the finite spaces for velocity and pressure are

$$\boldsymbol{W}_h := \{\boldsymbol{v}_h \in \boldsymbol{H}_{\text{div}}(\Gamma_h),\, \boldsymbol{v}_h \cdot \boldsymbol{n}_h = 0 \text{ on } \Gamma_h,\, \boldsymbol{v}_h \cdot \boldsymbol{\mu}_h = 0 \text{ on } \gamma_h^N,\, \boldsymbol{v}_h|_K \in \mathbb{RT}^0(K)\}$$
$$Q_h := \{q_h \in L^2(K) : q_h|_K \in \mathbb{P}^0(K)\},$$

where $\mathbb{RT}^0$ is the Raviart-Thomas finite elements space of lowest order degree. If $\left|\gamma^D\right| = 0$ to recover the uniqueness of the discrete solution, we consider the following discrete space for the pressure field

$$Q_h := \left\{q_h \in L^2(K) : q_h|_K \in \mathbb{P}^0(K)\right\} \cap L_0^2(\Gamma) \quad \text{with} \quad \|q\|_Q = \|q\|_{0,\Gamma},$$

otherwise the pressure is defined up to a constant.
We introduce the bilinear forms for the discrete problem, *i.e.* $a_h(\cdot,\cdot) : \boldsymbol{W}_h \times \boldsymbol{W}_h \to \mathbb{R}$ and $b_h(\cdot,\cdot) : \boldsymbol{W}_h \times Q_h \to \mathbb{R}$, defined as

$$a_h(\boldsymbol{u}_h, \boldsymbol{v}_h) := (\eta \boldsymbol{u}_h, \cdot \boldsymbol{v}_h)_{\Gamma_h} \quad \text{and} \quad b_h(\boldsymbol{v}_h, q_h) := -(q_h, \nabla_{\Gamma_h} \cdot \boldsymbol{v}_h)_{\Gamma_h},$$

and the linear functionals $F_h(\cdot) : Q_h \to \mathbb{R}$ and $G_h(\cdot) : \boldsymbol{W}_h \to \mathbb{R}$, given by

$$F_h(q_h) := -(f_h, q_h)_{\Gamma_h} \quad \text{and} \quad G_h(\boldsymbol{v}_h) := -\left(\hat{p}_h, \boldsymbol{v}_h \cdot \boldsymbol{\mu}_h\right)_{\partial\Gamma_h} + (\boldsymbol{g}_h, \boldsymbol{v}_h)_{\Gamma_h}.$$

where f_h, $\hat{p}_h$ and $\boldsymbol{g}_h$ are an approximation of the data problem on Γ_h and $\partial\Gamma_h$. We will see in the next section how to choose this approximation. Given the previous definitions the discrete problem is presented in Problem (2).

Problem 2 (Discrete weak formulation) *Given* η *as in* (3)*, find* $(\boldsymbol{u}_h, p_h) \in \boldsymbol{W}_h \times Q_h$ *such that*

$$\begin{cases} a_h(\boldsymbol{u}_h, \boldsymbol{v}_h) + b_h(\boldsymbol{v}_h, p_h) = G_h(\boldsymbol{v}_h) & \forall \boldsymbol{v}_h \in \boldsymbol{W}_h \\ b_h(\boldsymbol{u}_h, q_h) = F_h(q_h) & \forall q_h \in Q_h \end{cases}. \tag{7}$$

It can be easily proved that for Problem (2) all results presented in the previous section for the continuous problem are still valid.
In order to compare the exact solution defined on Γ with the discrete one, it is necessary to project the latter on Γ. As concerns scalar functions we adopt the choice presented in [9], *i.e.* to lift the functions $q_h \in Q_h$ as $\widetilde{q}_h(\boldsymbol{a}(\boldsymbol{x})) = q_h(\boldsymbol{x})$. This kind of lifting, however, does not work properly for the velocity field, in fact it does not map a function in $\boldsymbol{H}_{\text{div}}(\Gamma_h)$ in a function of $\boldsymbol{H}_{\text{div}}(\Gamma)$. In order to preserve this feature, we have to choose how to deal with the lifting of vectorial functions more carefully. We use the so called Piola transformation, refer to [19] for a more detailed presentation.

Definition 4.1 (Piola transformation) *Consider* $\Omega_0 \subset \mathbb{R}^n$ *and let* F *be a non degenerate map from* Ω_0 *to* $\Omega \subset \mathbb{R}^n$*. Let also be* $J = DF(\boldsymbol{X})$*, with* $J_{ij} = \partial F_i / \partial X_j$*, and* $\boldsymbol{\Psi} \in [L^2(\Omega_0)]^n$*. The Piola transformation* $\mathcal{F}$ *is then defined as*

$$\mathcal{F}(\boldsymbol{\Psi}) := \frac{1}{|\text{det} J|} J \boldsymbol{\Psi} \circ F^{-1}.$$

We now consider a triangle $K \in \Gamma_h$ and its projection on the surface Γ given by the curved triangle $\widetilde{K} = \{\boldsymbol{a}(\boldsymbol{x}) \in \Gamma : \boldsymbol{x} \in K\}$. We use a coordinate system local to the triangle K, so that a generic point $\hat{\boldsymbol{x}} \in K$ has coordinates $\hat{\boldsymbol{x}} = (\hat{x}_1, \hat{x}_2, 0)$. We define a map $\boldsymbol{\varphi} : K \to \widetilde{K}$ as

$$\boldsymbol{\varphi}(\hat{\boldsymbol{x}}) := \boldsymbol{\varphi}(\hat{x}_1, \hat{x}_2) := \hat{\boldsymbol{x}} - d(\hat{\boldsymbol{x}}) \boldsymbol{n}(\hat{\boldsymbol{x}}), \tag{8}$$

where d and $\boldsymbol{n}$ are the distance function and the normal in the new frame of reference.

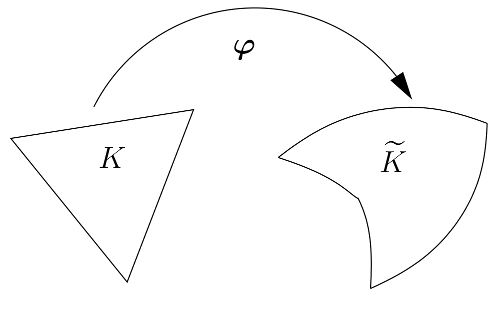

Figure 1: Maps from K to $\widetilde{K}$

We now extend $\boldsymbol{\varphi}$ to $\mathbb{R}^3$ introducing a new map $\boldsymbol{\Psi} : \mathbb{R}^3 \to \mathbb{R}^3$, defined as

$$\boldsymbol{\Psi}(\hat{\boldsymbol{x}}) := \boldsymbol{\varphi}(x_1, x_2) + x_3 \boldsymbol{n}(\hat{\boldsymbol{x}}). \tag{9}$$

The map $\boldsymbol{\Psi}$ is the one we consider for the construction of the Piola transformation.

The lifting of a scalar function $q_h : K \to \mathbb{R}$ to $\widetilde{q}_h : \widetilde{K} \to \mathbb{R}$ is therefore given by

$$\widetilde{q}_h(\boldsymbol{\Psi}(\hat{\boldsymbol{x}})) = q_h(\hat{\boldsymbol{x}}) \qquad \hat{\boldsymbol{x}} \in K. \tag{10}$$

Given $F := \nabla\boldsymbol{\Psi}$, the lifting of a vectorial function $\boldsymbol{w}_h : K \to \mathbb{R}^3$ to $\widetilde{\boldsymbol{w}}_h : \widetilde{K} \to \mathbb{R}^3$ is defined as

$$\widetilde{\boldsymbol{w}}_h(\boldsymbol{\Psi}(\hat{\boldsymbol{x}})) = \frac{1}{|\mathrm{det} F|} F\boldsymbol{w}_h(\hat{\boldsymbol{x}}) \qquad \hat{\boldsymbol{x}} \in K. \tag{11}$$

The matrix F has the following structure

$$F = [\boldsymbol{t}_1 \quad \boldsymbol{t}_2 \quad \boldsymbol{n}], \tag{12}$$

where $\boldsymbol{t}_i = \partial\boldsymbol{\varphi}/\partial x_i$, $i = 1, 2$ has components $\boldsymbol{t}_{i,j} = \delta_{ji} - n_j n_i - dH_{ji}$ for $j = 1, 2, 3$ with H the Hessian of the distance function d.

Remark 1 *It is immediate to show that* $\boldsymbol{t}_i \cdot \boldsymbol{n} = 0$ *for* $i = 1, 2$.

Since $d\sigma = |\boldsymbol{t}_1 \wedge \boldsymbol{t}_2| d\sigma_h$ and $\mathrm{det} F = (\boldsymbol{t}_1 \wedge \boldsymbol{t}_2) \cdot \boldsymbol{n}$ we have $d\sigma = \xi_h d\sigma_h$ where $\xi_h = |\mathrm{det} F|$.

Remark 2 *The matrix F is defined element wise. If we glue together all the local F, we find a global matrix that, to ease the notation, we will still indicate as F. In the following it will be clear from the domain of integration if we are referring to the local map or to the global one.*

We recall a useful lemma about the properties of the considered geometry. For a complete proof refer to [10].

Lemma 4.1 *Assume Γ and Γ_h defined as above. Then*

$$\|d\|_{L^\infty(\Gamma_h)} \leq ch^2.$$

Moreover, the quotient $\xi_h = d\sigma/d\sigma_h$ previously defined satisfies

$$\|1 - \xi_h\|_{L^\infty(\Gamma_h)} \leq ch^2.$$

We now deduce an important relationship between functions defined on K and their lifting on $\widetilde{K}$. We consider a couple of functions $(\boldsymbol{w}_h, q_h) \in \boldsymbol{W}_h \times Q_h$ and the corresponding lifting $(\widetilde{\boldsymbol{w}}_h, \widetilde{q}_h) \in \widetilde{\boldsymbol{W}}_h \times \widetilde{Q}_h$, where $\widetilde{\boldsymbol{W}}_h$ and $\widetilde{Q}_h$ are defined as

$$\widetilde{\boldsymbol{W}}_h := \left\{ \widetilde{\boldsymbol{w}}_h(\boldsymbol{x}) = \frac{1}{\xi_h} F\boldsymbol{w}_h \circ \boldsymbol{\Psi}^{-1}(\boldsymbol{x}),\, \boldsymbol{w}_h \in \boldsymbol{W}_h,\, \boldsymbol{x} \in \Gamma \right\},$$
$$\widetilde{Q}_h := \left\{ \widetilde{q}_h(\boldsymbol{x}) = q_h \circ \boldsymbol{\Psi}^{-1}(\boldsymbol{x}),\, q_h \in Q_h,\, \boldsymbol{x} \in \Gamma \right\}.$$

For such functions the following relation holds

$$\begin{aligned}(\nabla_\Gamma \cdot \widetilde{\boldsymbol{w}}_h, \widetilde{q}_h)_{\widetilde{K}} &= -(\widetilde{\boldsymbol{w}}_h, \nabla_\Gamma \widetilde{q}_h)_{\widetilde{K}} = -(\widetilde{\boldsymbol{w}}_h, (I - \boldsymbol{n} \otimes \boldsymbol{n}) \nabla \widetilde{q}_h)_{\widetilde{K}} \\ &= -\left(F\boldsymbol{w}_h, (I - \boldsymbol{n} \otimes \boldsymbol{n}) F^{-\top} \nabla q_h\right)_K \\ &= -\left(\boldsymbol{w}_h, F^\top (I - \boldsymbol{n} \otimes \boldsymbol{n}) F^{-\top} \nabla q_h\right)_K.\end{aligned}$$

In addition we have that

$$F^\top \boldsymbol{n} \otimes \boldsymbol{n} F^{-\top} = \begin{bmatrix} 0 & 0 & 0 \\ 0 & 0 & 0 \\ 0 & 0 & 1 \end{bmatrix} = \boldsymbol{e}_3 \otimes \boldsymbol{e}_3.$$

In the coordinate system local to K, $\boldsymbol{e}_3$ coincides with the normal $\boldsymbol{n}_h$ and so we have

$$F^\top \boldsymbol{n} \otimes \boldsymbol{n}\, F^{-\top} = \boldsymbol{n}_h \otimes \boldsymbol{n}_h.$$

Using this last relation we write that

$$\begin{aligned}(\nabla_\Gamma \cdot \widetilde{\boldsymbol{w}}_h, \widetilde{q}_h)_{\widetilde{K}} &= -(\boldsymbol{w}_h, (I - \boldsymbol{n}_h \otimes \boldsymbol{n}_h) \nabla q_h)_K \\ &= -(\boldsymbol{w}_h, \nabla_{\Gamma_h} q_h)_K = (\nabla_{\Gamma_h} \cdot \boldsymbol{w}_h, q_h)_K \\ &= \left(\frac{1}{\xi_h} \nabla_{\Gamma_h} \cdot \boldsymbol{w}_h, \widetilde{q}_h\right)_K.\end{aligned}$$

The last equality holds for all $\widetilde{q}_h \in \widetilde{Q}_h$ and so we can conclude that

$$\nabla_\Gamma \cdot \widetilde{\boldsymbol{w}}_h = \frac{1}{\xi_h} \nabla_{\Gamma_h} \cdot \boldsymbol{w}_h \qquad \text{a.e. in } \widetilde{K}. \tag{13}$$

Now we are able to prove the following

Lemma 4.2 *Given* $(\boldsymbol{w}_h, q_h) \in \boldsymbol{W}_h \times Q_h$ *and the corresponding lifting onto* Γ $(\widetilde{\boldsymbol{w}}_h, \widetilde{q}_h) \in \widetilde{\boldsymbol{W}}_h \times \widetilde{Q}_h$, *then exists some constants such that the following inequalities hold*

$$\begin{aligned}\frac{1}{C_1}\|q_h\|_{L^2(K)} \leq \|\widetilde{q}_h\|_{L^2(\widetilde{K})} \leq C_1 \|q_h\|_{L^2(K)} \\ \frac{1}{C_2}\|\boldsymbol{w}_h\|_{L^2(K)} \leq \|\widetilde{\boldsymbol{w}}_h\|_{L^2(\widetilde{K})} \leq C_2 \|\boldsymbol{w}_h\|_{L^2(K)} \\ \frac{1}{C_3}\|\nabla_{\Gamma_h} \cdot \boldsymbol{w}_h\|_{L^2(K)} \leq \|\nabla_\Gamma \cdot \widetilde{\boldsymbol{w}}_h\|_{L^2(\widetilde{K})} \leq C_3 \|\nabla_{\Gamma_h} \cdot \boldsymbol{w}_h\|_{L^2(K)}\end{aligned}$$

Proof. The first inequality is proved in [9]. For the second inequality we have by the definition of the L^2-norm

$$\|\widetilde{\boldsymbol{w}}_h\|^2_{L^2(\widetilde{K})} = (\widetilde{\boldsymbol{w}}_h, \widetilde{\boldsymbol{w}}_h)_{\widetilde{K}} = \left(\frac{1}{\xi_h} F^\top F \boldsymbol{w}_h, \boldsymbol{w}_h\right)_K.$$

Matrix $F^\top F$ is given by

$$F^\top F = \begin{bmatrix} |\boldsymbol{t}_1|^2 & \boldsymbol{t}_1 \cdot \boldsymbol{t}_2 & 0 \\ \boldsymbol{t}_1 \cdot \boldsymbol{t}_2 & |\boldsymbol{t}_2|^2 & 0 \\ 0 & 0 & 1 \end{bmatrix}.$$

From the definition of t_1 and t_2 it is straightforward that

$$|\boldsymbol{t}_i|^2 = 1 + \mathcal{O}(h^2) \quad \text{and} \quad \boldsymbol{t}_1 \cdot \boldsymbol{t}_2 \approx -n_1 n_2 + \mathcal{O}(h^2).$$

Following [10] we have that exists $c \in \mathbb{R}^+$ such that $\|n_i\|_{L^\infty(K)} \leq ch$, $i = 1, 2, 3$, then

$$\|\boldsymbol{t}_1 \cdot \boldsymbol{t}_2\|_{L^\infty(K)} \leq ch^2.$$

In conclusion the following inequality holds

$$\left\|I - F^\top F\right\|_{L^\infty(K)} \leq ch^2.$$

Thanks to this last relation and to lemma (4.1) the second estimate immediately follows. In order to prove the last inequality, using (13), we can write

$$\|\nabla_\Gamma \cdot \widetilde{\boldsymbol{w}}_h\|^2_{L^2(\widetilde{K})} = (\nabla_\Gamma \cdot \widetilde{\boldsymbol{w}}_h, \nabla_\Gamma \cdot \widetilde{\boldsymbol{w}}_h)_{\widetilde{K}} = \left(\frac{1}{\xi_h} \nabla_{\Gamma_h} \cdot \boldsymbol{w}_h, \nabla_\Gamma \cdot \widetilde{\boldsymbol{w}}_h\right)_K.$$

Using this relation and the estimate for ξ_h we can obtain the last inequality. □

5 Error analysis

In this section, to ease the analysis and the presentation of the forthcoming results, we consider fully homogeneous boundary conditions and zero vector source term. Thanks to the results of the previous section we can obtain the following useful relation

$$\int_{\widetilde{K}} \nabla_\Gamma \cdot \widetilde{\boldsymbol{w}}_h \, \widetilde{q}_h \, \mathrm{d}\sigma = \int_K \nabla_{\Gamma_h} \cdot \boldsymbol{w}_h \, q_h \, \mathrm{d}\sigma_h. \tag{14}$$

Therefore the approximation of the bilinear form $b(\cdot, \cdot)$ with $b_h(\cdot, \cdot)$ will not bring any additional error due to the discretization of the geometry. The additional term is only linked to the approximation of the bilinear form $a(\cdot, \cdot)$, in particular from

$$\int_K \eta \boldsymbol{u}_h \cdot \boldsymbol{v}_h \, \mathrm{d}\sigma_h = \int_{\widetilde{K}} \eta \xi_h \left(F^{-\top} F^{-1} \widetilde{\boldsymbol{u}}_h\right) \cdot \widetilde{\boldsymbol{v}}_h \, \mathrm{d}\sigma. \tag{15}$$

If we define $B_h := \xi_h F^{-\top} F^{-1}$ we can rewrite the discrete Problem 2 as

$$\begin{cases} (\eta B_h \widetilde{\boldsymbol{u}}_h, \widetilde{\boldsymbol{v}}_h)_\Gamma - (\widetilde{p}_h, \nabla_\Gamma \cdot \widetilde{\boldsymbol{v}}_h)_\Gamma = 0 & \forall \widetilde{\boldsymbol{v}}_h \in \widetilde{\boldsymbol{W}}_h, \\ (\widetilde{q}_h, \nabla_\Gamma \cdot \widetilde{\boldsymbol{u}}_h)_\Gamma = (f, q_h)_\Gamma & \forall \widetilde{q}_h \in \widetilde{Q}_h. \end{cases} \tag{16}$$

In this case we have chosen $f_h(\hat{\boldsymbol{x}}) = \xi_h f(\boldsymbol{\Psi}(\hat{\boldsymbol{x}}))$ in order to have $F_h = F$ on Γ.

Remark 3 *In practice is often simpler to compute the source term as* $f_h(\hat{\boldsymbol{x}}) = f(\boldsymbol{\Psi}(\hat{\boldsymbol{x}}))$*, thus adding an extra term of order* $\mathcal{O}(h^2)$ *to the error given by the difference between* f *and* F_h*.*

Lemma 5.1 *If* $(\boldsymbol{u}_h, p_h)$ *is solution of* (7)*, then its correspondent lift to* Γ*, indicated with* $(\widetilde{\boldsymbol{u}}_h, \widetilde{p}_h)$*, is solution of* (16) *and vice versa.*

Proof. Thanks to relations (14) and (15) we immediately get the equivalence between problems (7) and (16). $\square$

To provide an error estimate for our problem we need to recall some results on saddle-points problems, see [4, 18] for a detailed analyses. Introducing the following discrete functional space $\widetilde{\boldsymbol{W}}_h^f := \{\widetilde{\boldsymbol{w}}_h \in \widetilde{\boldsymbol{W}}_h : (\widetilde{q}_h, \nabla_\Gamma \cdot \widetilde{\boldsymbol{w}}_h - f)_\Gamma = 0 \ \forall \widetilde{q}_h \in \widetilde{Q}_h\}$, the Lemma 5.2 holds true [18].

Lemma 5.2 *If the spaces* $\widetilde{\boldsymbol{W}}_h$ *and* $\widetilde{Q}_h$ *satisfy the inf-sup condition then for each* $f \in L^2(\Gamma)$ *there exist a unique* $\widetilde{\boldsymbol{w}}_h^f \in (\widetilde{\boldsymbol{W}}_h^0)^\perp$ *such that:*

$$(\widetilde{q}_h, \nabla_\Gamma \cdot \widetilde{\boldsymbol{w}}_h^f - f)_\Gamma = 0 \quad \forall \widetilde{q}_h \in \widetilde{Q}_h \tag{17}$$

and

$$\left\| \widetilde{\boldsymbol{w}}_h^f \right\|_{\boldsymbol{W}} \leq \frac{1}{\beta} \sup_{\widetilde{q}_h \in \widetilde{Q}_h, \widetilde{q}_h \neq 0} \frac{(f, \widetilde{q}_h)_\Gamma}{\|\widetilde{q}_h\|_Q}. \tag{18}$$

Furthermore if $\widetilde{\boldsymbol{u}}_h \in \widetilde{\boldsymbol{W}}_h$ *satisfies*

$$(\eta B_h \widetilde{\boldsymbol{u}}_h, \widetilde{\boldsymbol{v}}_h)_\Gamma = 0 \quad \forall \widetilde{\boldsymbol{v}}_h \in \widetilde{\boldsymbol{W}}_h^0,$$

then there exists a unique $\widetilde{p}_h \in \widetilde{Q}_h$ *such that*

$$-(\widetilde{p}_h, \nabla_\Gamma \cdot \widetilde{\boldsymbol{v}}_h)_\Gamma + (\eta B_h \widetilde{\boldsymbol{u}}_h, \widetilde{\boldsymbol{v}}_h)_\Gamma = 0 \quad \forall \widetilde{\boldsymbol{v}}_h \in \widetilde{\boldsymbol{W}}_h \tag{19}$$

and

$$\|\widetilde{p}_h\|_{L^2} \leq \frac{1}{\beta} \sup_{\widetilde{\boldsymbol{v}}_h \in \widetilde{\boldsymbol{W}}_h, \widetilde{\boldsymbol{v}}_h \neq 0} \frac{(\eta B_h \widetilde{\boldsymbol{u}}_h, \widetilde{\boldsymbol{v}}_h)_\Gamma}{\|\widetilde{\boldsymbol{v}}_h\|_{\boldsymbol{W}}}. \tag{20}$$

By setting $\widetilde{\boldsymbol{u}}_h = \widetilde{\boldsymbol{u}}_h^0 + \widetilde{\boldsymbol{w}}_h^f$, with $\widetilde{\boldsymbol{u}}_h^0 \in \widetilde{\boldsymbol{W}}_h^0$ and $\widetilde{\boldsymbol{w}}_h^f \in \widetilde{\boldsymbol{W}}_h^f$, we can rewrite (16) as : find $\widetilde{u}_h^0 \in \widetilde{\boldsymbol{W}}_h^0$ such that:

$$\left(\eta B_h \widetilde{\boldsymbol{u}}_h^0, \widetilde{\boldsymbol{v}}_h\right)_\Gamma = -\left(\eta B_h \widetilde{\boldsymbol{w}}_h^f, \widetilde{\boldsymbol{v}}_h\right)_\Gamma \quad \forall \widetilde{\boldsymbol{v}}_h \in \widetilde{\boldsymbol{W}}_h^0. \tag{21}$$

Thanks to the Lax-Milgram Theorem, it exists a unique solution $\widetilde{\boldsymbol{u}}_h^0 \in \widetilde{\boldsymbol{W}}_h^0$ of (21) which satisfies $\|\widetilde{\boldsymbol{u}}_h^0\|_{\boldsymbol{W}} \leq C \|\widetilde{\boldsymbol{w}}_h^f\|_{L^2}$, for a $C > 0$. Then, from (18) and (20) we have:

$$\|\widetilde{\boldsymbol{u}}_h\|_{\boldsymbol{W}} \leq \frac{C}{\beta} \|f\|_{L^2} \quad \text{and} \quad \|\widetilde{p}_h\|_{L^2} \leq \frac{C}{\beta} \|\widetilde{\boldsymbol{u}}_h\|_{L^2}.$$

To find an estimate for the discretization error we write (16) in the following form, which highlights the classical saddle point structure:

$$\begin{cases} (\eta\widetilde{\boldsymbol{u}}_h, \widetilde{\boldsymbol{v}}_h)_\Gamma - (\widetilde{p}_h, \nabla_\Gamma \cdot \widetilde{\boldsymbol{v}}_h)_\Gamma = (\eta(I - B_h)\widetilde{\boldsymbol{u}}_h, \widetilde{\boldsymbol{v}}_h)_\Gamma & \forall \widetilde{\boldsymbol{v}}_h \in \widetilde{\boldsymbol{W}}_h, \\ (\widetilde{q}_h, \nabla_\Gamma \cdot \widetilde{\boldsymbol{u}}_h)_\Gamma = (f, q_h)_\Gamma & \forall \widetilde{q}_h \in \widetilde{Q}_h. \end{cases} \tag{22}$$

By subtracting (1) and (22) and adding and subtracting to the result a vector $\widetilde{\boldsymbol{w}}_h^* \in \widetilde{\boldsymbol{W}}_h^f$, we obtain

$$(\eta(\widetilde{\boldsymbol{u}}_h - \widetilde{\boldsymbol{w}}_h^*), \widetilde{\boldsymbol{v}}_h)_\Gamma + (p - \widetilde{p}_h, \nabla_\Gamma \cdot \widetilde{\boldsymbol{v}}_h)_\Gamma = (\eta(\widetilde{\boldsymbol{u}} - \widetilde{\boldsymbol{w}}_h^*), \widetilde{\boldsymbol{v}}_h)_\Gamma + (\eta(I - B_h)\widetilde{\boldsymbol{u}}_h, \widetilde{\boldsymbol{v}}_h)_\Gamma$$

By choosing $\widetilde{\boldsymbol{v}}_h = \widetilde{\boldsymbol{u}}_h - \widetilde{\boldsymbol{w}}_h^*$, with $\widetilde{\boldsymbol{v}}_h \in \widetilde{\boldsymbol{W}}_h$, and using (5), we get:

$$\|\widetilde{\boldsymbol{v}}_h\|_{\boldsymbol{W}} \leq C\left(\|\widetilde{\boldsymbol{u}} - \widetilde{\boldsymbol{w}}_h^*\|_{L^2} + \|I - B_H\|_{L^\infty}\|f\|_{L^2}\right),$$

from which it follows that

$$\|\widetilde{\boldsymbol{u}} - \widetilde{\boldsymbol{u}}_h\|_{\boldsymbol{W}} \leq C\left(\inf_{\widetilde{\boldsymbol{w}}_h^* \in \widetilde{\boldsymbol{W}}_h^f} \|\widetilde{\boldsymbol{u}} - \widetilde{\boldsymbol{w}}_h^*\|_{\boldsymbol{W}} + \|I - B_H\|_{L^\infty}\|f\|_{L^2}\right).$$

Now we want to show that

$$\inf_{\widetilde{\boldsymbol{w}}_h^* \in \widetilde{\boldsymbol{W}}_h^f} \|\widetilde{\boldsymbol{u}} - \widetilde{\boldsymbol{w}}_h^*\|_{\boldsymbol{W}} \leq C \inf_{\widetilde{\boldsymbol{v}}_h \in \widetilde{\boldsymbol{W}}_h} \|\widetilde{\boldsymbol{u}} - \widetilde{\boldsymbol{v}}_h\|_{\boldsymbol{W}}. \tag{23}$$

From Lemma 5.2, for all $\widetilde{\boldsymbol{v}}_h \in \widetilde{\boldsymbol{W}}_h$, there exists a unique $\widetilde{\boldsymbol{z}}_h \in (\widetilde{\boldsymbol{W}}_h^0)^\perp$ such that

$$(\widetilde{q}_h, \nabla_\Gamma \cdot \widetilde{\boldsymbol{z}}_h)_\Gamma = (\widetilde{q}_h, \nabla_\Gamma \cdot (\boldsymbol{u} - \widetilde{\boldsymbol{v}}_h))_\Gamma \quad \forall \widetilde{q}_h \in Q_h,$$

and $\|\widetilde{\boldsymbol{z}}_h\|_{\boldsymbol{W}} \leq C\|\nabla_\Gamma \cdot (\boldsymbol{u} - \widetilde{\boldsymbol{v}}_h)\|_{L^2}$. Setting $\widetilde{\boldsymbol{w}}_h^* = \widetilde{\boldsymbol{z}}_h + \widetilde{\boldsymbol{v}}_h$, we have $\widetilde{\boldsymbol{w}}_h^* \in \widetilde{\boldsymbol{W}}_h^f$ and we obtain $\|\boldsymbol{u} - \widetilde{\boldsymbol{w}}_h^*\|_{\boldsymbol{W}} \leq \|\boldsymbol{u} - \widetilde{\boldsymbol{v}}_h\|_{\boldsymbol{W}}$, from which (23) follows.
Repeating a similar analysis for the pressure, we get the final inequality

$$\begin{aligned} \|\boldsymbol{u} - \widetilde{\boldsymbol{u}}_h\|_{\boldsymbol{W}} + \|p - \widetilde{p}_h\|_Q \leq C\Bigg(&\|I - B_h\|_{L^\infty}\|f\|_{L^2} + \\ &+ \inf_{\widetilde{\boldsymbol{v}}_h \in \widetilde{\boldsymbol{W}}_h} \|\boldsymbol{u} - \widetilde{\boldsymbol{v}}_h\|_{\boldsymbol{W}} + \inf_{\widetilde{q}_h \in \widetilde{Q}_h} \|p - \widetilde{q}_h\|_Q\Bigg). \end{aligned} \tag{24}$$

In (24) we observe that, as we expected, the error is composed by two different terms, the first related to the finite element discretization and the second related to the approximation of the geometry of the problem. In particular, as seen in the previous section for $F^\top F$, we can immediately conclude that

$$\|I - B_h\|_{L^\infty(\Gamma)} \leq ch^2.$$

Thus the contribution of the geometric error in a Darcy problem is of the second order respect to grid size h.
We prove the main result of this section.

Theorem 5.1 (Order of convergence) *Let $(\boldsymbol{u}, p) \in \boldsymbol{W} \times Q$ be the solution of the continuous problem (4), $(\boldsymbol{u}_h, p_h) \in \boldsymbol{W}_h \times Q_h$ the solution of the discrete problem (7) and $(\widetilde{\boldsymbol{u}}_h, \widetilde{p}_h) \in \widetilde{\boldsymbol{W}}_h \times \widetilde{Q}_h$ its corresponding lift to Γ. Assuming that the solution is regular enough and that $\xi_h \in H^1(K)$, then the following inequality holds*

$$\|\boldsymbol{u} - \widetilde{\boldsymbol{u}}_h\|_{\boldsymbol{W}} + \|p - \widetilde{p}_h\|_Q \leq Ch \left(\|\nabla_\Gamma \cdot \boldsymbol{u}\|_{H^1(\Gamma)} + \|\boldsymbol{u}\|_{H^1(\Gamma)} + |p|_{H^1(\Gamma)} \right).$$

Proof. If we neglect in (24) the geometric contribution to the error, we have

$$\|\boldsymbol{u} - \widetilde{\boldsymbol{u}}_h\|_{\boldsymbol{W}} + \|p - \widetilde{p}_h\|_Q \leq \left(\inf_{\boldsymbol{w}_h \in \widetilde{\boldsymbol{W}}_h} \|\boldsymbol{u} - \widetilde{\boldsymbol{w}}_h\|_{\boldsymbol{W}} + \inf_{\widetilde{q}_h \in \widetilde{Q}_h} \|p - \widetilde{q}_h\|_Q \right)$$

We start considering the estimate for the velocity field and we introduce the function $\hat{\boldsymbol{u}} : \Gamma_h \to \mathbb{R}^3$, defined as follows

$$\hat{\boldsymbol{u}}(\hat{\boldsymbol{x}}) := \xi_h \, F^{-1} \boldsymbol{u}(\Psi(\hat{\boldsymbol{x}})) \quad \text{with} \quad \hat{\boldsymbol{x}} \in \Gamma_h.$$

So $\hat{\boldsymbol{u}}$ is the projection of the exact solution on discrete surface. Thanks to lemma (4.2) we have

$$\|\boldsymbol{u} - \widetilde{\boldsymbol{w}}_h\|_{\boldsymbol{H}_{\text{div}}(\widetilde{K})} \leq \|\hat{\boldsymbol{u}} - \boldsymbol{w}_h\|_{\boldsymbol{H}_{\text{div}}(K)},$$

This relation, together with standard results for $\boldsymbol{H}_{\text{div}}$, gives us

$$\|\boldsymbol{u} - \widetilde{\boldsymbol{w}}_h\|_{\boldsymbol{H}_{\text{div}}(\widetilde{K})} \leq Ch_k \left(|\nabla_{\Gamma_h} \cdot \hat{\boldsymbol{u}}|_{H^1(K)} + |\hat{\boldsymbol{u}}|_{\boldsymbol{H}_{\text{div}}(K)} \right).$$

We see now how to estimate the right hand side of the inequality. From the definition of the H^1 semi-norm it follows that

$$|\nabla_{\Gamma_h} \cdot \hat{\boldsymbol{u}}|^2_{H^1(K)} = \|\nabla_{\Gamma_h}(\nabla_{\Gamma_h} \cdot \hat{\boldsymbol{u}})\|^2_{L^2(K)} = (\nabla_{\Gamma_h}(\nabla_{\Gamma_h} \cdot \hat{\boldsymbol{u}}), \nabla_{\Gamma_h}(\nabla_{\Gamma_h} \cdot \hat{\boldsymbol{u}}))_K.$$

From [11] and (13) we obtain $\nabla_{\Gamma_h}(\nabla_{\Gamma_h} \cdot \hat{\boldsymbol{u}}) = P_h(I - dH)\nabla_\Gamma(\xi_h \nabla_\Gamma \cdot \boldsymbol{u})$, that inserted in the semi-norm definition gives us

$$|\nabla_{\Gamma_h} \cdot \hat{\boldsymbol{u}}|^2_{H^1(K)} = (A_h \nabla_\Gamma(\xi_h \nabla_\Gamma \cdot \boldsymbol{u}), \nabla_\Gamma(\xi_h \nabla_\Gamma \cdot \boldsymbol{u}))_K,$$

where A_h is defined as $A_h := P(I - dH)P_h(I - dH)P/\xi_h$. We know that ξ_h^{-1} is bounded and moreover, from [9], we have

$$P(I - dH)P_h(I - dH)P \approx PP_hP + \mathcal{O}(h^2).$$

That becomes

$$PP_hP = P - (\boldsymbol{n}_h - (\boldsymbol{n}_h \cdot \boldsymbol{n})\boldsymbol{n})(\boldsymbol{n}_h - (\boldsymbol{n}_h \cdot \boldsymbol{n})\boldsymbol{n})^\top.$$

Because in the reference system local to the triangle K, we have $\boldsymbol{n}_h = \boldsymbol{e}_3$, then

$$|\boldsymbol{n}_h - (\boldsymbol{n}_h \cdot \boldsymbol{n})\boldsymbol{n}| = |\boldsymbol{e}_3 - n_3\boldsymbol{n}| = \sqrt{1 - n_3^2} = \sqrt{n_1^2 + n_2^2} \approx \mathcal{O}(h).$$

Therefore for matrix A_h holds the relation $A_h \approx P + \mathcal{O}(h^2)$, Moreover, thanks to the regularity of the surface P is bounded and so it is A_h. Then we can obtain

$$|\nabla_{\Gamma_h} \cdot \hat{\boldsymbol{u}}|_{H^1(K)} \leq \|A_h\|^{\frac{1}{2}}_{L^\infty(\widetilde{K})} \|\nabla_\Gamma(\xi_h \nabla_\Gamma \cdot \boldsymbol{u})\|_{L^2(\widetilde{K})}$$

Applying triangular and Schwarz's inequalities

$$\begin{aligned}\|\nabla_\Gamma(\xi_h \nabla_\Gamma \cdot \boldsymbol{u})\|_{L^2(\widetilde{K})} \leq \|\nabla_\Gamma \xi_h\|_{L^2(\widetilde{K})} \|\nabla_\Gamma \cdot \boldsymbol{u}\|_{L^2(\widetilde{K})} + \\ + \|\xi_h\|_{L^2(\widetilde{K})} \|\nabla_\Gamma(\nabla_\Gamma \cdot \boldsymbol{u})\|_{L^2(\widetilde{K})} \leq C^* \|\nabla_\Gamma \cdot \boldsymbol{u}\|_{H^1(\widetilde{K})},\end{aligned}$$

where $C^* = \max\left\{\|\nabla_\Gamma \xi_h\|_{L^2(\widetilde{K})}, \|\xi_h\|_{L^2(\widetilde{K})}\right\}$. Defining $C_1 = C^* \|A_h\|^{\frac{1}{2}}_{L^\infty(\widetilde{K})}$, we have proved that

$$|\nabla_{\Gamma_h} \cdot \hat{\boldsymbol{u}}|_{H^1(K)} \leq C_1 \|\nabla_\Gamma \cdot \boldsymbol{u}\|_{H^1(\widetilde{K})}. \tag{25}$$

In analogous way we can show the following inequality for the semi-norm

$$|\hat{\boldsymbol{u}}|_{H^1(K)} \leq C_2 \|\boldsymbol{u}\|_{H^1(\widetilde{K})}. \tag{26}$$

Summing (25) and (26) over all triangles we obtain the velocity estimate. We consider now the estimate for pressure and, similarly to what we have done for velocity, we introduce the lift of the exact solution p to Γ_h as

$$\hat{p}(\hat{\boldsymbol{x}}) := p(\Psi(\hat{\boldsymbol{x}})) \quad \text{with} \quad \hat{\boldsymbol{x}} \in \Gamma_h.$$

From lemma (4.2) and from standard interpolation results we have

$$\|p - \widetilde{q}_h\|_{L^2(\widetilde{K})} \leq C\|\hat{p} - q_h\|_{L^2(K)} \leq C_3 h_K \, |\hat{p}|_{H^1(K)}\,.$$

Finally we exploit the results of [9] and we obtain

$$\|p - \widetilde{q}_h\|_{L^2(\widetilde{K})} \leq C C_3 h_K \, |p|_{H^1(\widetilde{K})}\,.$$

Considering the contribution of all the elements we have the desired estimation for the pressure. □

6 Applicative examples

We present in the following sub-sections some examples to show the goodness of the proposed approximation. In particular we show the error convergence for two different geometries: a sphere and a toroid. The choice is driven by the analytical solutions proposed in the literature for these geometries. The results are in good agreement with the theory. The simulations we propose in this paper are performed using the library for finite elements LifeV [14] developed by École Polytechnique Fédérale de Lausanne (CMCS), Politecnico di Milano (MOX), INRIA under the projects REO and ESTIME and Emory University (Math&CS). Finally to ensure that the geometrical error is small enough and to increase the accurateness of the numerical solution, we have used the software presented in [7] to increase the grids quality.

6.1 Order of convergence

We consider problem (2) solved on two different domains Γ_1 and Γ_2, where the former is a unit sphere while the latter a spherical cup limited by $\theta \in [-\pi/2, \pi/2]$ and $\phi \in [0, 2\pi]$. A unit permeability is considered and the scalar source term is taken as $f(\theta, \phi) = 2(2\cos^2\theta - \sin^2\theta)$ such that the exact solution is $p(\theta, \phi) = \cos^2\theta$. For Γ_1 the problem does not require boundary condition, hence to have a well-posed problem we impose the solution in one point. While for Γ_2 we consider Dirichlet boundary conditions equal to the exact solution. The advantage of using a spherical domain, in addition to the use of spherical coordinate in finding the exact solution, is that we explicitly know the distance function $d(\boldsymbol{x}) = |\boldsymbol{x}| - 1$.

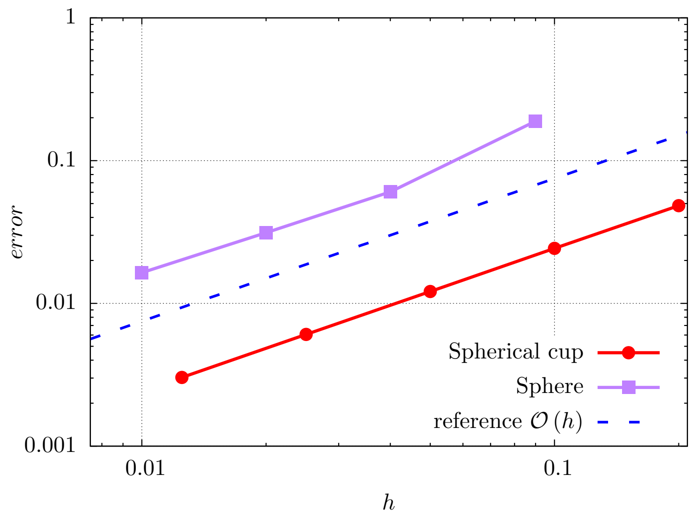

Figure 2: Error decay for the sphere and the spherical cup compared with a reference curve of $\mathcal{O}(h)$.

In Figure 2 we present the error history, for the two problems, decreasing the mesh thickness. It is clear that in both cases the error obtained scales at least as $\mathcal{O}(h)$, confirming the theoretical result presented in Theorem 5.1. Observing the solutions reported in Figure 3, for the sphere, and in Figure 4, for the spherical cup, we can notice that the velocity field obtained is tangent to the surface and flows in the opposite direction of the pressure gradient, as we expect from the Darcy's law.

6.2 Example 2

In this second example we consider as surface a torus defined by

$$\Gamma = \left\{ (x, y, z) \in \mathbb{R}^3 : \left(\sqrt{x^2 + y^2} - 1 \right)^2 + z^2 - 0.6^2 = 0 \right\}.$$

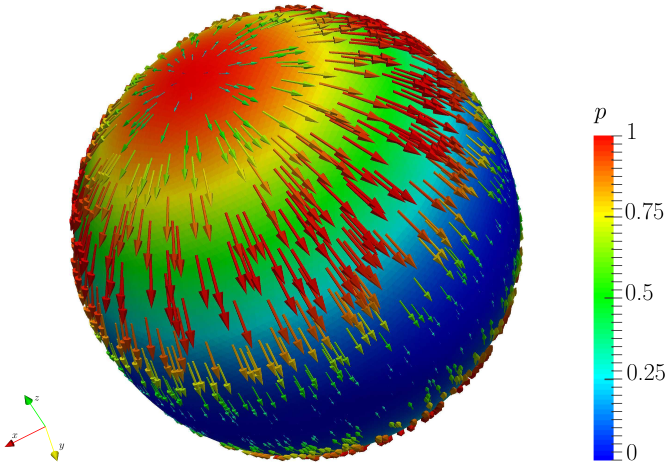

Figure 3: Numerical solution on the unit sphere. Both pressure and velocity are represented. The arrows for the latter are coloured and sized as the velocity magnitude. We can notice that the in the two poles of the sphere and in its equator the pressure change slowly so does the velocity.

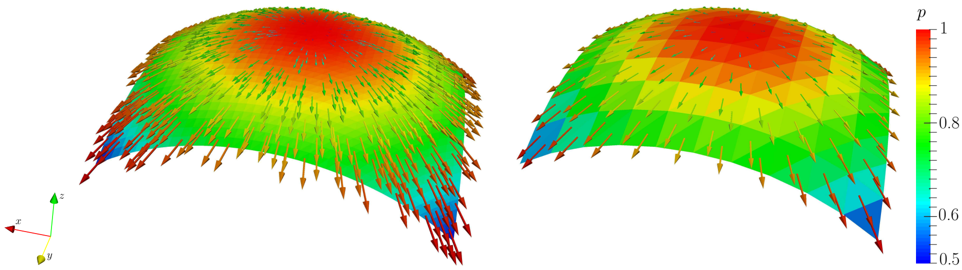

(a) Solution for a fine mesh (b) Solution for a coarse mesh

Figure 4: Numerical solution on a spherical cup of a unit sphere. Both pressure and velocity are represented. The arrows for the latter are coloured and sized as the velocity magnitude. We can see that the solution is more smooth refining the mesh.

The exact solution for the pressure, expressed in toroidal coordinates, is given by $p(\phi, \theta) = \sin(3\phi)\cos(3\theta + \phi)$, and the correspondent source term is equal to $f(\phi, \theta) = \frac{1}{r^2}(9\sin(3\phi)\cos(3\theta + \phi)) - \frac{1}{(R-r\cos(\theta))^2}(-10\sin(3\phi)\cos(3\theta + \phi) - 6\cos(3\phi)\sin(3\theta + \phi)) - \frac{1}{r(R-r\cos(\theta))}(3\sin(\phi)\sin(3\phi)\sin(3\theta + \phi))$, where $r = 0.6$ and $R = 1$. As in the previous case a unique solution is obtained by imposing the exact solution in one point. In Figure 5 we can observe that, also in this

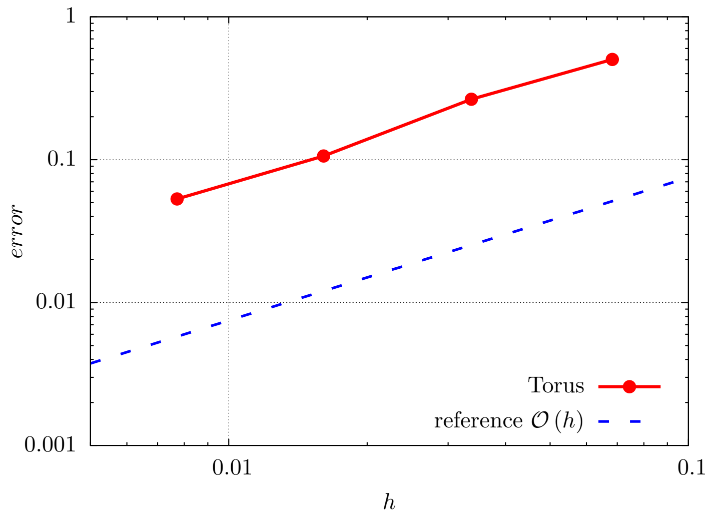

Figure 5: Error decay for the torus compared with a reference curve of $\mathcal{O}(h)$.

example, the decay of the error confirms the results presented in the theory. Figure 6 shows the obtained solution.

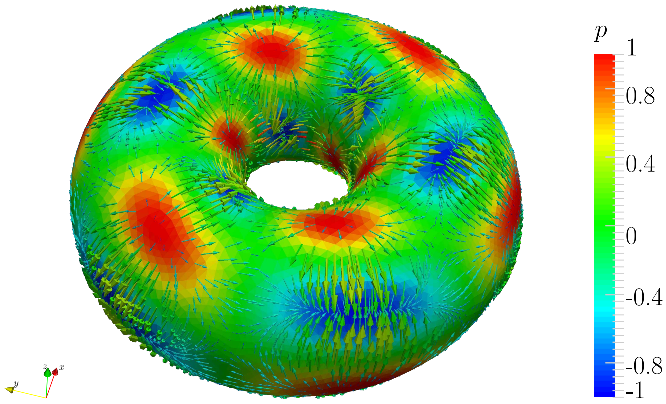

Figure 6: Numerical solution on the torus. Both pressure and velocity are represented. The arrows for the latter are coloured and sized as the velocity magnitude.

7 Conclusions

In this work we have presented a framework to solve Darcy problems on regular manifolds. The numerical discretization chosen is the classical pair of piecewise constant, for the pressure, and lowest order tangential Raviart-Thomas, for the Darcy velocity, finite element spaces. In this context we have provided an analysis of the relations between the quantities defined on the real surface and the ones defined on its discretization. Then we have used this properties in order to prove some results for the convergence of the approximation error. The numerical experiments proposed have confirmed the estimate presented in the theory.
A possible development, following the reduced model proposed in [17, 6, 16, 13, 15], of the work could be the application of the results obtained in more realistic cases, for example in solving the Darcy problem defined in a whole basin. In such a case we should introduce suitable coupling conditions between the domain and the reduced model of the fracture and, in the case of a network of fractures, we should provide models for the flow along the intersecting curves.

8 Acknowledgements

The authors wish to thank Antonio Cervone, Franco Dassi, Guido Iori and Anna Scotti for many fruitful discussions.

References

[1] Paola F. Antonietti, Andreas Dedner, Pravin Madhavan, Simone Stangalino, Björn Stinner, and Marco Verani. High order discontinuous galerkin methods on surfaces. Technical report, Politecnico di Milano, 2014.

[2] Jacob Bear. *Dynamics of Fluids in Porous Media.* American Elsevier, 1972.

[3] Marcelo Bertalmío, Li-Tien Cheng, Stanley Osher, and Guillermo Sapiro. Variational problems and partial differential equations on implicit surfaces. *Journal of Computational Physics*, 174(2):759–780, 2001.

[4] Franco Brezzi and Michel Fortin. *Mixed and Hybrid Finite Element Methods*, volume 15 of *Computational Mathematics.* Springer Verlag, Berlin, 1991.

[5] Chris D. Cantwell, Sergey Yakovlev, Robert M. Kirby, Nicholas S. Peters, and Spencer J. Sherwin. High-order spectral/*hp* element discretisation for reaction-diffusion problems on surfaces: Application to cardiac electrophysiology. *J. Comput. Phys.*, 257:813–829, January 2014.

[6] Carlo D'Angelo and Anna Scotti. A mixed finite element method for Darcy flow in fractured porous media with non-matching grids. *Mathematical Modelling and Numerical Analysis*, 46(02):465–489, 2012.

[7] Franco Dassi, Simona Perotto, Luca Formaggia, and Paolo Ruffo. Efficient geometric reconstruction of complex geological structures. *Mathematics and Computers in Simulation*, 2014.

[8] Alan Demlow and Gerhard Dziuk. An adaptive finite element method for the Laplace-Beltrami operator on implicitly defined surfaces. *SIAM Journal on Numerical Analysis*, 45(1):421–442, 2007.

[9] Gerhard Dziuk. Finite elements for the beltrami operator on arbitrary surfaces. In Stefan Hildebrandt and Rolf Leis, editors, *Partial Differential Equations and Calculus of Variations*, volume 1357 of *Lecture Notes in Mathematics*, pages 142–155. Springer Berlin Heidelberg, 1988.

[10] Gerhard Dziuk and Charles M Elliott. Finite elements on evolving surfaces. *IMA journal of numerical analysis*, 27(2):262–292, 2007.

[11] Gerhard Dziuk and Charles M Elliott. Surface finite elements for parabolic equations. *Journal of Computational Mathematics*, 25(4), 2007.

[12] Alexandre Ern and Jean-Luc Guermond. *Theory and practice of finite elements*. Applied mathematical sciences. Springer, 2004.

[13] Luca Formaggia, Alessio Fumagalli, Anna Scotti, and Paolo Ruffo. A reduced model for Darcy's problem in networks of fractures. *ESAIM: Mathematical Modelling and Numerical Analysis*, 48:1089–1116, 7 2014.

[14] Gilles Fourestey and Simone Deparis. Lifev user manual. `http://lifev.org`, November 2010.

[15] Alessio Fumagalli and Anna Scotti. A numerical method for two-phase flow in fractured porous media with non-matching grids. *Advances in Water Resources*, 62, Part C(0):454–464, 2013. Computational Methods in Geologic CO2 Sequestration.

[16] Alessio Fumagalli and Anna Scotti. An efficient xfem approximation of darcy flow in arbitrarly fractured porous media. *Oil and Gas Sciences and Technologies - Revue d'IFP Energies Nouvelles*, April 2014.

[17] Vincent Martin, Jérôme Jaffré, and Jean E. Roberts. Modeling fractures and barriers as interfaces for flow in porous media. *SIAM J. Sci. Comput.*, 26(5):1667–1691, 2005.

[18] Alfio Quarteroni and Alberto Valli. *Numerical approximation of partial differential equations*, volume 23 of *Springer Series in Computational Mathematics*. Springer-Verlag, Berlin, 1994.

[19] Marie E Rognes, Robert C Kirby, and Anders Logg. Efficient assembly of h(div) and h(curl) conforming finite elements. *SIAM Journal on Scientific Computing*, 31(6):4130–4151, 2009.

MOX Technical Reports, last issues

Dipartimento di Matematica "F. Brioschi",
Politecnico di Milano, Via Bonardi 9 - 20133 Milano (Italy)

30/2014 Ferroni, A.; Formaggia, L.; Fumagalli, A.;
Numerical analysis of Darcy problem on surfaces

29/2014 Arioli, G.; Koch, H.
Some symmetric boundary value problems and non-symmetric solutions

28/2014 Antonietti, P; Panfili, P.; Scotti, A.; Turconi, L. ; Verani, M.; Cominelli,A.; Formaggia,L.
Optimal techniques to simulate flow in fractured reservoirs

27/2014 Vergara, C; Domanin, M; Guerciotti, B; Lancellotti, R.M.; Azzimonti, L; Forzenigo, L; Pozzoli, M
Computational comparison of fluid-dynamics in carotids before and after endarterectomy

26/2014 Discacciati, M.; Gervasio, P.; Quarteroni, A.
Interface Control Domain Decomposition (ICDD) Methods for Heterogeneous Problems

25/2014 Hron, K.; Menafoglio, A.; Templ, M.; Hruzova K.; Filzmoser, P.
Simplicial principal component analysis for density functions in Bayes spaces

24/2014 Ieva, F., Jackson, C.H., Sharples, L.D.
Multi-State modelling of repeated hospitalisation and death in patients with Heart Failure: the use of large administrative databases in clinical epidemiology

23/2014 Ieva, F., Paganoni, A.M., Tarabelloni, N.
Covariance Based Unsupervised Classification in Functional Data Analysis

22/2014 Arioli, G.
Insegnare Matematica con Mathematica

21/2014 Artina, M.; Fornasier, M.; Micheletti, S.; Perotto, S.
The benefits of anisotropic mesh adaptation for brittle fractures under plane-strain conditions